# A Positive Regulator of Nodule Organogenesis, NODULE INCEPTION, Acts as a Negative Regulator of Rhizobial Infection in *Lotus japonicus*[1][W]

**Emiko Yoro, Takuya Suzaki, Koichi Toyokura, Hikota Miyazawa, Hidehiro Fukaki, and Masayoshi Kawaguchi***

Division of Symbiotic Systems, National Institute for Basic Biology, Okazaki, Aichi 444–8585, Japan (E.Y., T.S., M.K.); Department of Basic Biology, School of Life Science, Graduate University for Advanced Studies, Okazaki, Aichi 444–8585, Japan (E.Y., T.S., M.K.); Department of Biology, Graduate School of Science, Kobe University, Kobe 657–8501, Japan (K.T., H.F.); and Research Faculty of Agriculture, Hokkaido University, Sapporo 060–8589, Japan (H.M.)

Legume-rhizobium symbiosis occurs in specialized root organs called nodules. To establish the symbiosis, two major genetically controlled events, rhizobial infection and organogenesis, must occur. For a successful symbiosis, it is essential that the two phenomena proceed simultaneously in different root tissues. Although several symbiotic genes have been identified during genetic screenings of nonsymbiotic mutants, most of the mutants harbor defects in both infection and organogenesis pathways, leading to experimental difficulty in investigating the molecular genetic relationships between the pathways. In this study, we isolated a novel nonnodulation mutant, *daphne*, in *Lotus japonicus* that shows complete loss of nodulation but a dramatically increased numbers of infection threads. Characterization of the locus responsible for these phenotypes revealed a chromosomal translocation upstream of *NODULE INCEPTION* (*NIN*) in *daphne*. Genetic analysis using a known *nin* mutant revealed that *daphne* is a novel *nin* mutant allele. Although the *daphne* mutant showed reduced induction of *NIN* after rhizobial infection, the spatial expression pattern of *NIN* in epidermal cells was broader than that in the wild type. Overexpression of *NIN* strongly suppressed hyperinfection in *daphne*, and *daphne* phenotypes were partially rescued by cortical expression of *NIN*. These observations suggested that the *daphne* mutation enhanced the role of NIN in the infection pathway due to a specific loss of the role of NIN in nodule organogenesis. Based on these results, we provide evidence that the bifunctional transcription factor NIN negatively regulates infection but positively regulates nodule organogenesis during the course of the symbiosis.

Legumes develop a specialized symbiotic organ on their roots, the root nodule, in response to rhizobial infection. Benefiting from symbiotic nitrogen fixation by rhizobia in the nodule, plants can grow under nitrogen-limited conditions. The signaling pathways in nodule development are divided into two major events, rhizobial infection and organogenesis. For a successful symbiotic association, it is essential that the two phenomena proceed simultaneously in different root tissues (Crespi and Frugier, 2008; Madsen et al., 2010; Oldroyd, 2013). Rhizobial infection occurs in the epidermal cells of the root. Rhizobia penetrate the root tissues from curled root hair cells and progress toward the root cortex through an intracellular channel called the infection thread (IT; Vasse and Truchet, 1984; Gage, 2004; Jones et al., 2007; Fournier et al., 2008; Murray, 2011). In contrast, organogenesis begins with the reinitiation of cell division in the root cortex. Several nonnodulation or low-nodulation mutants have been identified by genetic mutant screening in the model legumes *Lotus japonicus* and *Medicago truncatula*. Those mutants are impaired in rhizobial infection processes at different steps, from earlier steps (root hair deformation and bacterial colonization; e.g. *Lotus japonicus nod factor receptor5* (*Ljnfr5*)/*Medicago truncatula nod factor perception* (*Mtnfp*), *Lotus japonicus symbiosis receptor kinase* (*Ljsymrk*)/*Medicago truncatula doesn't make infections2* (*Mtdmi2*), *Lotus japonicus calcium- and calmodulin-dependent protein kinase* (*Ljccamk*)/*Medicago truncatula doesn't make infections3* (*Mtdmi3*)) to later steps (IT initiation, IT progression, and bacterial release; e.g. *Lotus japonicus cyclops* (*Ljcyclops*)/*Medicago truncatula interacting protein of DMI3* (*Mtipd3*) *and Lotus japonicus cerberus* (*Ljcerberus*)/*Medicago truncatula lumpy infections* (*Mtlin*); Kouchi et al., 2010; Popp and Ott, 2011). The respective mutated genes are involved in each event. These genes show diverse spatial expression patterns in the epidermis, cortex, and nodule (Popp and Ott, 2011). This complexity has made it difficult to elucidate the

[1] This work was supported by the Ministry of Education, Culture, Sports, Science, and Technology of Japan (Grants-in-Aid for Scientific Research nos. 23012038 to T.S. and 22128006 to M.K.) and the Yoshida Scholarship Foundation (to E.Y.).

* Address correspondence to masayosi@nibb.ac.jp.

The author responsible for distribution of materials integral to the findings presented in this article in accordance with the policy described in the Instructions for Authors (www.plantphysiol.org) is: Masayoshi Kawaguchi (masayosi@nibb.ac.jp).

[W] The online version of this article contains Web-only data.
www.plantphysiol.org/cgi/doi/10.1104/pp.113.233379

  

molecular mechanism of the interrelationship between the two major signaling pathways of nodule development, occurring in both the epidermis and cortex at different developmental stages.

A few reports have recently focused on the cross talk or independence of these two pathways, using different approaches. By characterization of the phenotypes of various double mutant/transgenic plants harboring 14 individual infection-defective mutations and three spontaneous-nodule-formation mutations/transgenes, symbiotic genes in *L. japonicus* were categorized into four groups (Madsen et al., 2010): (1) genes for only infection, such as *NAK-associated protein1* (*NAP1*), *121F-specific p53-inducible RNA* (*PIR1*), and *CERBERUS*; (2) genes for organogenesis and indirectly for infection, such as *SymRK*, *NUCLEOPORIN85*, and *POLLUX*; (3) genes for both infection and organogenesis, such as *NODULE INCEPTION* (*NIN*), *NODULATION SIGNALING PATHWAY1* (*NSP1*), and *NSP2*; and (4) genes for cross talk between infection and organogenesis, such as *CCaMK* and *CYCLOPS*. Another study of expression systems under the control of a tissue-specific promoter investigated the special contributions of *MtNFP/LjNFR5* and *MtDMI3/LjCCaMK* to IT formation and nodule organogenesis in a tissue-autonomous manner (Rival et al., 2012). A third study of *LjsymRK* mutant alleles proposed different contributions of LjSYMRK to each pathway depending on different domains (Kosuta et al., 2011). These studies have shown that the SYMRK-CCaMK-CYCLOPS signaling cascade has two roles: rhizobial infection in the epidermis and nodule organogenesis in the root cortex. However, the tissue-specific roles or cellular interactions between the epidermal event and the inner tissue event of transcription factors functioning in later symbiotic signaling, such as NIN, NSP1, and NSP2, remain unclear.

Among the nonnodulation mutants, the *nin* mutant is defective in both IT initiation and nodule formation. It is believed that *NIN*, a transcription factor containing

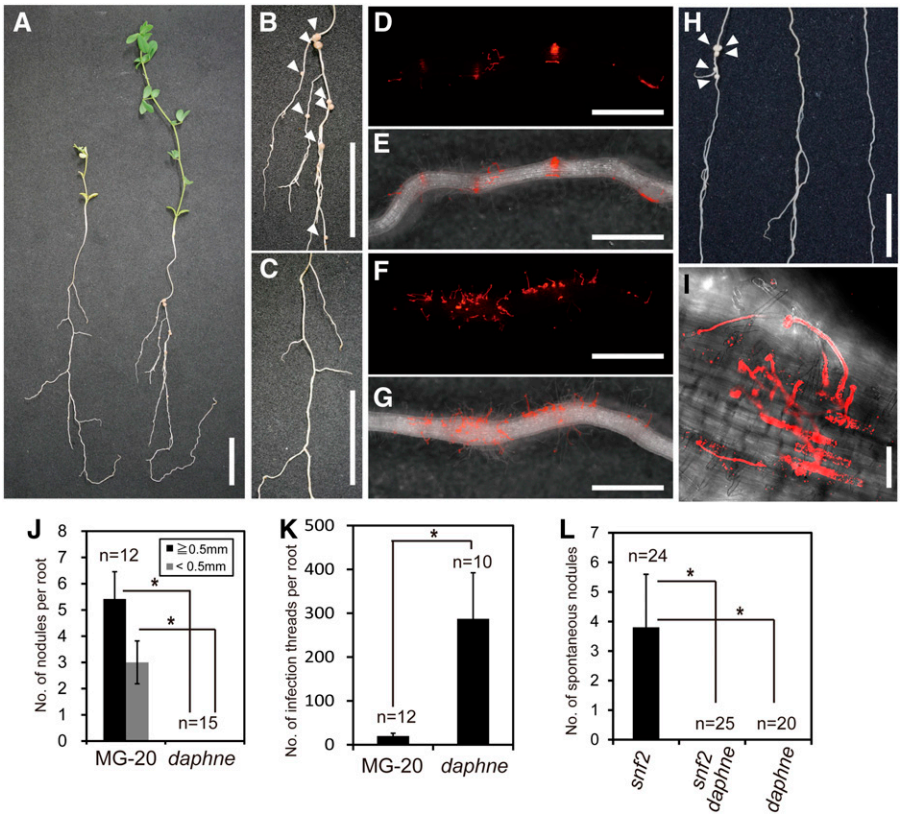


**Figure 1.** Isolation of a novel nonnodulation mutant, *daphne*. A, Shoot and root phenotypes of the *daphne* mutant (left) and the Miyakojima MG-20 wild type (right) at 28 DAI. B, Nodulation phenotype of Miyakojima MG-20. Arrowheads indicate nodules. C, The nonnodulation phenotype of *daphne*. D to G, IT formation of the Miyakojima MG-20 root (D and E) and of the *daphne* root (F and G) following inoculation with *M. loti* MAFF303099 constitutively expressing *DsRED*. D and F, Red fluorescence images of roots. Linear red signals indicate ITs. E and G, Red fluorescence images and transmitted light images are merged. H, Spontaneous nodule formation in *snf2* (left), the *daphne snf2* double mutant (middle), and *daphne* (right). Arrowheads indicate spontaneous nodules. I, Confocal microscopic image of a *daphne* root. Z-stack series are shown in Supplemental Figure S2. Bars = 2 cm in A to C and H and 1 mm in D to G. J, Nodules were counted at 28 DAI with *M. loti* MAFF303099. K, The number of ITs per root was counted at 7 DAI with *M. loti* MAFF303099 constitutively expressing *LacZ*. L, Six weeks after germination, spontaneous nodules were counted without rhizobial infection under the no-nitrogen condition. Error bars indicate SD. $^*P < 0.05$ by Student's *t* test.

an RWP-RK domain which is named after a conserved motif, functions in both the infection and organogenesis pathways (Schauser et al., 1999; Borisov et al., 2003; Marsh et al., 2007). The expression pattern of the *GUS* reporter gene driven by the *NIN* promoter (*ProNIN*) indicates that epidermal expression a short time after inoculation is correlated with rhizobial infection, whereas expression in the root cortex at a later stage contributes to cell division (Heckmann et al., 2011; Kosuta et al., 2011; Popp and Ott, 2011). *NIN* transcription is highly induced only after rhizobial inoculation, and constitutive expression of *NIN* can lead to the ectopic division of cortical cells in the absence of rhizobia. These results indicate that NIN plays a central role in nodule organogenesis (Schauser et al., 1999; Tirichine et al., 2007; Suzaki et al., 2012; Soyano et al., 2013).

Cytokinin also plays an important role in nodule organogenesis, given that a loss-of-function mutation in the putative cytokinin receptors LOTUS HISTIDINE KINASE1 (LHK1) in *L. japonicus* and the knockdown of CYTOKININ RESPONSE1 in *M. truncatula* cause the low-nodulation phenotypes (Gonzalez-Rizzo et al., 2006; Murray et al., 2007). In contrast, the *spontaneous nodule formation2* (*snf2*) mutant, which has a gain-of-function mutation in LHK1, yields a spontaneous nodulation phenotype in *L. japonicus* (Tirichine et al., 2007). Likewise, ectopic cortical cell division and *NIN* expression are induced by exogenous cytokinin application without

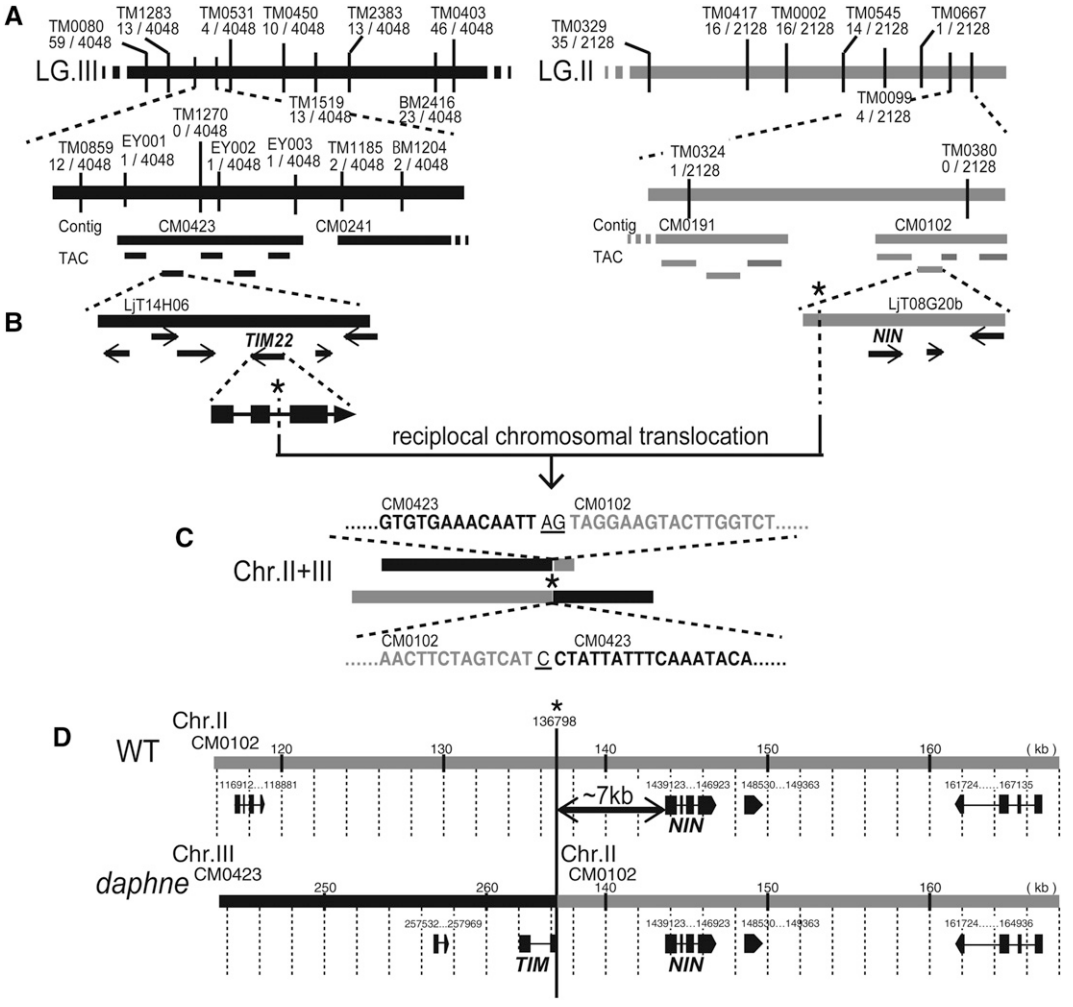


**Figure 2.** Identification of the *daphne* mutation. A, Two genetic linkage maps of the regions of *daphne* loci in linkage group (LG) III (black, left) and linkage group II (gray, right). The newly developed marker (EY001-3) is shown in Supplemental Table S2. The number of recombination events (events/total chromosomes) is indicated. B, Physical maps of transformation-competent artificial chromosome (TAC) clone LjT14H06 (black, left) and TAC clone LjT08G20b (gray, right). Arrows indicate the annotations from miyakogusa.jp release 2.5 (http://www.kazusa.or.jp/lotus/; Sandal et al., 2006). C, Outline of chromosomal translocation between chromosome (Chr.) II and chromosome III, with sequences at the fusion point identified by inverse PCR amplified from the *daphne* genome. Black letters indicate the bases from CM0423 (chromosome III), and gray letters indicate the bases from CM0102 (chromosome II). Bases of unknown chromosomal origin are indicated by underlined letters. D, The locations of translocation fusion points in the contigs with gene annotations (exons shown as block boxes and introns shown as thin lines). Numbers on the ruler indicate the exact points (kb) in each contig. WT, Wild type. Asterisks indicate the reciprocal chromosomal translocation points of each locus.

rhizobial infection (Gonzalez-Rizzo et al., 2006; Murray et al., 2007; Heckmann et al., 2011). Cytokinin activates the cortical expression of *NIN* but does not induce the epidermal expression of *NIN*, suggesting that cytokinin activates only the organogenesis pathway and not the infection pathway mediated by NIN (Heckmann et al., 2011).

In this study, we identified a novel *nin* mutant allele, named *daphne*, which showed the interesting phenotypes of nonnodulation and hyper IT formation in *L. japonicus*. The mutant showed an altered expression pattern of *NIN*. In view of the relationship between the spatiotemporal expression pattern of *NIN* and the symbiotic phenotype of *daphne*, we propose a new cellular communication model controlled by NIN involving cross talk between infection and organogenesis for regulating rhizobial infection processes.

## RESULTS

### Isolation of the *daphne* Mutant, Which Showed Nonnodulation and Dramatically Increased Infection of Rhizobia in *L. japonicus*

To date, several host genes necessary for nodule development have been identified (Madsen et al., 2010; Oldroyd, 2013). However, most nonnodulation mutants have defects in both the rhizobial infection and organogenesis pathways, so the molecular relationship between these two pathways and the mechanisms for controlling each pathway have remained obscure. To find new components involved in the infection or organogenesis pathways, we first screened ion-beam-mutagenized *L. japonicus* seeds of accession Miyakojima MG-20 (3,400 M1 lines) for the nonnodulation mutants. We next evaluated their infection ability. As a final step, we focused on a mutant, named *daphne*, displaying the novel phenotype of nonnodulation and hyperinfection. The *daphne* mutant was completely defective in nodule formation, being different from *hyper infected1* (*hit1*), which was previously isolated as a hyperinfection mutant able to form a few nodules (Supplemental Fig. S1; Murray et al., 2007). In the *daphne* mutant, no nodules were observed even 28 d after inoculation (DAI; Fig. 1, A–C and I). *daphne* showed a typical nonnodulation phenotype, with pale-yellow leaves and growth delay under low-nitrogen conditions (Fig. 1A). However, in *daphne*, the number of ITs per root was dramatically increased, to 15-fold greater than that on the MG-20 wild type (Fig. 1, D–G and J). In the wild type, ITs tend to be formed in small restricted regions called susceptible zones (Vasse et al., 1993; Penmetsa and Cook, 1997; Krusell et al., 2002; Gage, 2004). On the other hand, ITs were observed on almost all regions of *daphne* roots. This extended rhizobial susceptibility has been observed previously in the *nin* mutant

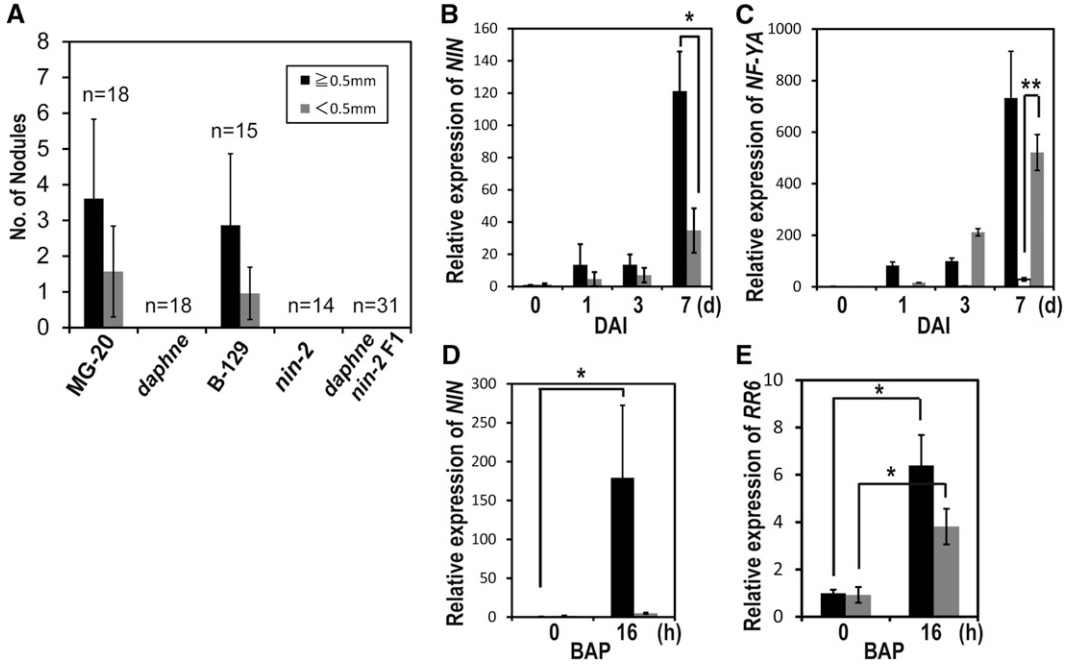


**Figure 3.** *daphne* is a novel *nin* mutant allele. A, Allelism tests by crossing *daphne* and *nin-2* mutants (Schauser et al., 1999). Nodules were counted at 14 DAI on each plant root. B to E, Quantitative real-time RT-PCR analysis of *NIN* (B and D), *NF-YA* (C), and *RR6* (E) expression in the Miyakojima MG-20 wild type (black bars), in *daphne* (gray bars), and in *nin-9* (white bars) noninoculated (0), at 1, 3, and 7 DAI (B and C), or dependent on cytokinin treatment ($10^{-7}$ M benzylaminopurine [BAP]) for 16 h (D and E). Each cDNA was prepared from total RNA derived from whole root. Fold changes in expression are shown relative to roots at 0 DAI (B and C) or before cytokinin treatment (D and E). Error bars indicate SD of three biological replicates. $^{*}P < 0.05$, $^{**}P < 0.01$ by Student's *t* test.

(Schauser et al., 1999). Additionally, IT elongation in *daphne* was visible in root hair but aborted and burst in the epidermal cell layer, and no cortical ITs were observed (Fig. 1I; Supplemental Fig. S2).

To identify the step of the organogenesis pathway that is blocked in *daphne*, we created the *daphne snf2* double mutant and evaluated its ability for spontaneous nodule formation. *snf2* has a gain-of-function mutation in the *LHK1* gene, which encodes a cytokinin receptor protein. In this mutant, only genes downstream of cytokinin signaling are constitutively active. Accordingly, *snf2* can form a nodule-like structure without rhizobial infection (Tirichine et al., 2007). The nonspontaneous nodule formation phenotype of the *daphne snf2* double mutant indicates that the nonnodulation phenotype of *daphne* is caused by defects downstream of cytokinin signaling (Fig. 1, H and K).

### Identification of the *daphne* Mutation by Map-Based Cloning and Inverse PCR

We roughly identified two loci on chromosomes II and III linked to the nonnodulation phenotype of *daphne* using a small F2 mapping population by map-based cloning (http://www.kazusa.or.jp/lotus/; Sandal et al., 2006; Supplemental Fig. S3). This result was apparently inconsistent with the observation that the F2 population segregated in an approximately 3:1 ratio, indicating that *daphne* is a recessive mutant. (Supplemental Table S1). We further explored the locus using a large F2 population with markers on linkage group III, and the translocation fusion point was identified by reverse transcription (RT)-PCR (Fig. 2; Supplemental Fig. S4). We finally detected the fused sequences, which originated from chromosomes II and III in the *daphne* genome, by inverse PCR. This finding suggested that the ion beam irradiation had induced a reciprocal chromosomal translocation. The translocation points lie in the second intron of the *Translocase of the inner membrane* (*TIM*) gene (chr3.CM0423.360.r2.d) on chromosome III and in an intergenic region (IGR) on chromosome II. The IGR sequence on the IGR lies approximately 7 kb upstream of *NIN*, which is known to be an essential gene for nodule development (Schauser et al., 1999). No mutation in the *NIN* coding region was detected in the *daphne* genome.

### *daphne* Is a Novel *nin* Mutant Allele, Different from the *nin* Null Mutant

As described above, we determined two candidate loci responsible for the nonnodulation phenotype in *daphne*: *TIM*, on chromosome III, and *NIN*, on chromosome II. Although we introduced the coding sequence of *TIM* gene under the control of the ubiquitin promoter (*ProLjUBQ*; Maekawa et al., 2008) by hairy root transformation, the nonnodulation phenotype was not complemented (Supplemental Fig. S4). We next hypothesized that a translocation near the *NIN* locus causes the *daphne* phenotype, a notion supported by the previous characterization of a *nin* mutant that displays nonnodulation and no IT formation (Schauser et al., 1999). By crossing *daphne* (accession Miyakojima MG-20) and *nin-2* (accession Gifu B-129), we tested whether *daphne* is a *nin* mutant allele. The success of crossing experiments using pollen of *nin-2* was judged by the accumulation of anthocyanin, the dominant characteristic phenotype of Gifu B-129 (*nin-2*), in stems. All *daphne* × *nin-2* F1 plants originating from three independent seed

**Table I.** *Phenotypic effects of the expression of the NIN or NIN chimeric repressor in the MG-20 wild type, daphne, and nin*

*J0571>>NIN* rescued the nonnodulation phenotype. *ProLjUBQ::NIN* and *J0571>>NIN* inhibited hyperinfection in *daphne*. *ProLjUBQ::NIN::SRDX* showed the repression of both nodulation in MG-20 and infection in *daphne*. *ProNIN::NIN::TerNIN* rescued no infection phenotype of *nin*, yielding that the *NIN* promoter used in this study shows sufficient expression pattern at least for the infection pathway. Important results are highlighted in boldface.

| Plant Genotype | Transgene | Nodule | | | abLR[b] | IT | | | Total Plants |
|---|---|---|---|---|---|---|---|---|---|
| | | + | Low[a] | − | | ++[c] | Low[d] | − | |
| MG-20 | *ProLjUBQ::GUS* | 20 | 0 | 0 | 0 | 0 | 20 | 0 | 20 |
| | *ProLjUBQ::NIN* | 19 | 0 | 0 | 10 | 0 | 19 | 0 | 19 |
| | *ProLjUBQ::NIN::SRDX* | **5** | **7** | **6** | 5 | 0 | 18 | 0 | 18 |
| | *J0571>>mCherry-NLS* | 20 | 0 | 0 | 0 | 0 | 20 | 0 | 20 |
| | *J0571>>NIN* | 20 | 0 | 0 | 3 | 0 | 20 | 0 | 20 |
| *daphne* | *ProLjUBQ::GUS* | 0 | 0 | 18 | 0 | 18 | 0 | 0 | 18 |
| | *ProLjUBQ:NIN* | 0 | 0 | 20 | 4 | **0** | **18** | **2** | 20 |
| | *ProLjUBQ:NIN::SRDX* | 0 | 0 | 19 | 2 | **3** | **14** | **2** | 19 |
| | *J0571>>mCherry-NLS* | 0 | 0 | 25 | 0 | 25 | 0 | 0 | 25 |
| | *J0571>>NIN* | **6** | **0** | **17** | 6 | 13 | 10 | 0 | 23 |
| *nin-9* | *ProLjUBQ::GUS* | 0 | 0 | 15 | 0 | 0 | 0 | 15 | 15 |
| | *ProLjUBQ:NIN* | 0 | 0 | 14 | 5 | 0 | 0 | 6 | 6 |
| | *ProNIN::NIN::TerNIN* | 0 | 0 | 14 | 0 | 0 | **10** | **4** | 14 |
| | *J0571>>NIN* | 0 | 0 | 22 | 2 | 0 | 0 | 22 | 22 |

[a]Roots with small size and number of nodules (Supplemental Fig. S7). [b]Roots with aberrant lateral root such as enlarged tips and bumps (Supplemental Fig. S6). [c]Roots with the typical *daphne* phenotype, highly increased IT number. [d]Roots with the wild-type-like infection phenotype, normal IT number.

pods exhibited nonnodulation (Fig. 3A). These results suggested that *daphne* and *nin-2* are allelic for the nonnodulation phenotype. Although the normal infection phenotype of *daphne* × wild-type F1 plants and the F2 segregation ratio indicate that both *daphne* phenotypes, nonnodulation and hyperinfection, are recessive (Supplemental Table S1), *daphne* × *nin-2* F1 plants showed hyperinfection. We also observed that the excessive root hair deformation phenotype in *daphne* was similar to the phenotype of the *nin* mutant (Supplemental Fig. S5). For the subsequent analysis described below, we used *nin-9* (Suzaki et al., 2012) as a canonical *nin* mutant because it has the same genetic background as *daphne*.

### *daphne* Has Completely Lost the *NIN* Expression Induced by Cytokinin Application

NIN is a putative key transcription factor that plays a role in the infection and nodule organogenesis pathways. The expression level of *NIN* is strongly elevated in an inoculation-dependent manner (Schauser et al., 1999). Because the allelism test showed that *daphne* was a *nin* mutant allele, we next investigated the *NIN* expression pattern in *daphne*. Expression in whole roots was slightly induced by inoculation with *Mesorhizobium loti*. The transcript levels of *NIN* at earlier stages were almost identical in the wild type and *daphne*, whereas at 7 DAI, the level of *NIN* expression in *daphne* was almost one-third that in the wild type (Fig. 3B). The induction level of *Nuclear transcription factor Y alpha* (*NF-YA*), known as a downstream target of NIN (Soyano et al., 2013), also indicates that *daphne* partially retains the function of NIN, compared with almost no induction of *NF-YA* in a typical *nin* mutant, *nin-9* (Fig. 3C).

We next evaluated the cytokinin-induced expression level of *NIN*, finding it to be completely absent in *daphne* (Fig. 3D). This loss is in good agreement with the finding that the *snf2* mutation spontaneously activating the cytokinin signal does not rescue the nonnodulation phenotype of *daphne* (Fig. 1, H and K), because cytokinin is believed to induce only the organogenesis pathway and not the infection pathway (Heckmann et al., 2011). The cytokinin-induced expression of *Lotus japonicus RESPONSE REGULATOR6* (*RR6*; Op den Camp et al., 2011) was detected even in *daphne*, suggesting that *daphne* retains the cytokinin responsiveness of genes other than *NIN* (Fig. 3E).

### *daphne* Shows Broad Epidermal Expression Patterns of *NIN*

How is the lower expression of *NIN* in the *daphne* mutant implicated in the increased number of ITs? To identify the underlying mechanism of increased infection events, we investigated the spatial expression pattern of *NIN*. We cloned approximately 4 kb of *ProNIN* and approximately 2 kb of the *NIN* terminator (*TerNIN*) for promoter-*GUS* analysis. For 10 of 14 *nin-9* plants, their IT formation was rescued by introducing the *ProNIN*::*NIN*::*TerNIN* construct. This indicated that the *NIN* promoter was sufficient for the function of NIN at least as involved in rhizobial infection (Table I; Supplemental Fig. S5). In the wild type, blue staining was restricted to several small epidermal regions of the root (Fig. 4, A, C, and E), as reported previously (Radutoiu et al., 2003; Kosuta et al., 2011). The inner cells of nodule primordia in the wild type were also stained, as observed previously (Fig. 4I; Heckmann et al., 2011). In contrast, we observed a broad range, almost the whole root area, of *NIN* promoter activity in the *daphne* root (Fig. 4, B, D, and F). The broader activity of *ProNIN*::*GUS*::*TerNIN* in *daphne* coincided with the region where excessive root hair curling and IT formation occur (Fig. 4, A–H).

### Overexpression of NIN Strongly Represses the Hyperinfection in *daphne*

The above result showed that *daphne* exerts broad *ProNIN* activity in the epidermis, indicating a broader susceptible

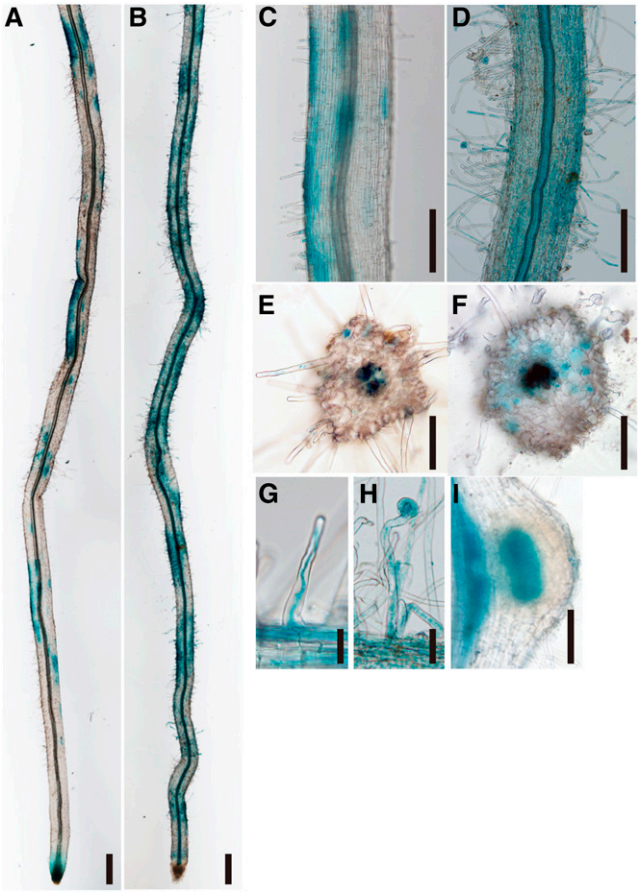


**Figure 4.** Spatial expression analysis of the *NIN* gene. GUS staining images of *Agrobacterium rhizogenes*-mediated transformed roots with *ProNIN*::*GUS*::*TerNIN* at 7 DAI (with the *M. loti* MAFF303099 wild type) on the Miyakojima MG-20 wild type (A, C, E, and G) and *daphne* (B, D, F, and H). Blue staining was observed with transformed (GFP-positive) hairy roots in susceptible zones (A–F), including root hair cells (G and H) and an immature nodule in the wild type (I). Bars = 0.5 mm in A to D and 0.1 mm in E to I.

zone for rhizobial infection than in the wild type. Based on these results, we hypothesized that NIN itself negatively regulates rhizobial infection. To address the negative function, we accordingly overexpressed *NIN* under the control of *ProLjUBQ* in *daphne* roots and observed the IT formation phenotype with *M. loti* expressing *DsRED*. Surprisingly, the hyperinfection phenotype of *daphne* was strongly suppressed in *NIN*-overexpressing transgenic roots, whereas *GUS*-overexpressing roots and nontransformed (GFP-negative) roots retained the excessive IT formation phenotype (Fig. 5, A–C and I–K; Table I). The hyperinfection phenotype of nontransformed roots indicates that the negative feedback regulation of IT formation is not long-distance signaling mediated by the shoot, in contrast to the regulation of the number of nodules (Okamoto et al., 2009). We also observed no normal nodules, but some lateral roots with enlarged tips and bumps, in *ProLjUBQ*::*NIN* transgenic roots in *daphne* (Table I; Supplemental Fig. S6; Suzaki et al., 2012; Soyano et al., 2013).

Next, we confirmed the positive function of NIN in rhizobial infection in the *daphne* mutant background. We expressed a chimeric protein of NIN and the SRDX domain, a transcriptional repressor domain in the Arabidopsis (*Arabidopsis thaliana*) SUPERMAN repressor (Oshima et al., 2011). *ProLjUBQ*:*NIN*::*SRDX* dominantly repressed the target gene expression of *NIN* in the MG-20 wild type, causing a reduction in the number of nodules (Table I; Supplemental Fig. S7). In *daphne*, the ITs almost disappeared only in *ProLjUBQ*:*NIN*::*SRDX*-expressing transgenic roots (Fig. 5, D, H, and J; Table I), phenocopying the previously observed phenotype of a typical *nin* mutant (Schauser et al., 1999; Marsh et al., 2007). This suggests that *daphne* maintains the positive function of NIN in rhizobial infection, unlike a typical *nin* mutant.

These results indicate that NIN plays not only positive but also negative roles in IT formation, and *daphne* maintains the positive role but loses the negative role. In contrast to *daphne*, MG-20 wild-type plants formed a low number of ITs (less than 20 per root; Fig. 1J), which may account for the observation that *ProLjUBQ*:*NIN* apparently had no strong suppressive effects on IT number in the wild type (Table I).

### Cortical But Not Epidermal Expression of *NIN* Was Specifically Lost in *daphne*

Both positive and negative roles of NIN in rhizobial infection have now been demonstrated. To further investigate the underlying mechanism, we hypothesized that the positive and negative actions of NIN are generated by epidermis and cortex, respectively, given that the lack of cytokinin-induced NIN in *daphne* results in an increase in the number of ITs and a typical *nin* mutant does not form ITs. We speculated that a less negative role of NIN in IT formation (cytokinin-induced NIN) resulted in excessive IT formation.

To address the tissue-specific activity of NIN, we attempted to express *NIN* using a cortex- and endodermis-specific enhancer isolated from Arabidopsis J0571

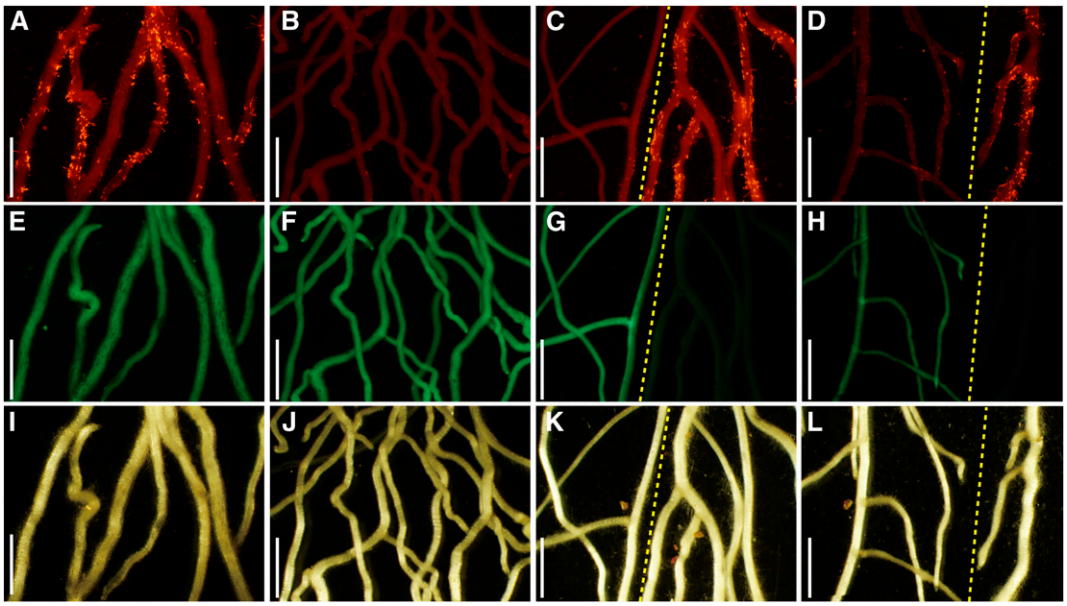


**Figure 5.** Ectopic expression of the *NIN* gene strongly suppresses excessive IT formation in *daphne*. Red fluorescence images (A–D), GFP fluorescence images (E–H), and transmitted light images (I–L) of *A. rhizogenes*-mediated transformed *daphne* roots are shown at 21 DAI. Roots were transformed with negative control vector *ProLjUBQ*::*GUS* (A, E, and I), *ProLjUBQ*::*NIN* (B, C, F, G, J, and K), or *ProLjUBQ*::*NIN*::*SRDX* (D, H, and L). ITs were observed by inoculating *M. loti* MAFF303099 constitutively expressing *DsRED* (A–D). GFP fluorescence showed transformed roots (E–H). Yellow dashed lines indicate the border between transformed and nontransformed roots. Bars = 2 cm.

(Miyashima et al., 2011). The J0571 enhancer element was identified from the Arabidopsis GAL4-GFP enhancer-trap lines (http://www.plantsci.cam.ac.uk/haseloff; http://www.arabidopsis.org/abrc/haseloff.jsp). First, we tested the fluorescent marker (*mCherry*-with nuclear localization signal [*NLS*]) expressed by *J0571* in hairy roots of *L. japonicus*. Although no marker expression was detected in the epidermis, signal was detected in the inner layers of the root, including cortex and endodermis (Supplemental Fig. S8), suggesting that the cortex- and endodermis-specific expression of *J0571* is conserved in *L. japonicus*. Both the nonnodulation phenotype and excessive IT formation in *daphne* were partially rescued by *J0571>>NIN* (Fig. 6; Table1), confirming that the *daphne* phenotype was caused by the loss of *NIN* expression specifically in the cortex.

## DISCUSSION

*NIN* was first identified as a gene responsible for the nonnodulation phenotype in legumes (Schauser et al., 1999). Since then, it has been believed that NIN, a putative transcription factor, plays a positive role in nodule organogenesis and IT formation. Meanwhile, the possibility has been discussed that NIN also has a negative role in the rhizobial infection processes, based on the excessive root hair response or the expanded *Early nodulin11* expression pattern in *nin* mutants and the lower expression of *NIN* in another hyper-IT mutant, *hit1-1* (Schauser et al., 1999; Marsh et al., 2007; Murray et al., 2007). In this study, we identified the *daphne* mutant, a novel *nin* mutant allele displaying excessive IT formation as well as nonnodulation. The spatiotemporal expression patterns of the *NIN* gene in *daphne* provided new evidence of negative feedback regulation of the infection process mediated by NIN. In *daphne*, the level of *NIN* transcription from whole roots was less than that in the wild type. In contrast, the epidermal expression of *NIN* was broader than that in the wild type, indicating that the susceptible zone for rhizobial infection was enlarged in *daphne*. This increased susceptibility for infection could account for the excessive IT formation in *daphne*. Furthermore, although overexpression of *NIN* suppressed excessive infection, inner cell layer-specific expression of *NIN* rescued nodule formation in *daphne*. Based on these observations, we propose a negative feedback regulation of rhizobial infection mediated by NIN (Fig. 7). In this model, NIN plays two important roles, one in infection and the other in organogenesis. NIN functioning in infection is located in the epidermis in an earlier stage (in the susceptible zone) for proceeding with IT formation, whereas NIN functioning in organogenesis acts in a later stage. NIN functioning in organogenesis has not only a positive role in promoting cell division in the cortex but also a negative role in inhibiting rhizobial infection. In *daphne*, owing to the loss of expression of such NIN functioning in organogenesis, the root area for rhizobial infection becomes

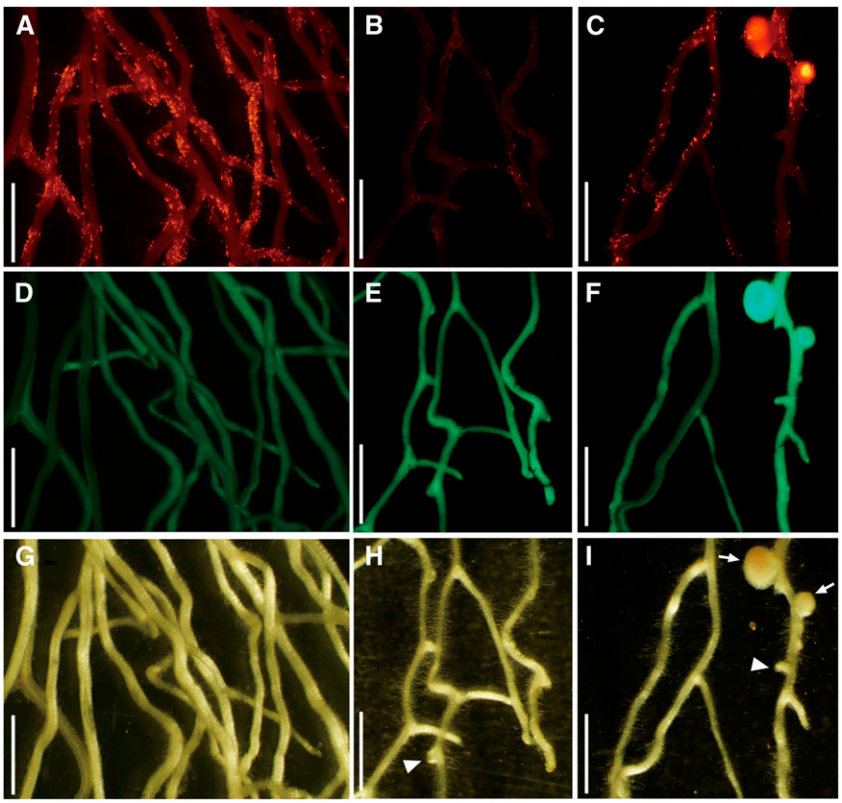


**Figure 6.** The nonnodulation phenotype in *daphne* is partially rescued by the cortical expression of *NIN*. Red fluorescence images (A–C), GFP fluorescence images (D–F), and transmitted light images (G–I) of *A. rhizogenes*-mediated transformed *daphne* roots are shown at 21 DAI. Roots were transformed with *J0571>>NIN* (A–I). Excessive ITs (A, D, and G), strongly suppressed ITs (B, E, and H), and nodules (C, F, and I) were observed by inoculating *M. loti* MAFF303099 constitutively expressing *DsRED*. GFP fluorescence showed transformed roots (D–F). Arrows and arrowheads indicate nodules and enlarged bumps, respectively. Bars = 2 cm.

broader. Several reports have already suggested that genes downstream of cytokinin signaling or *NIN* itself are involved in preserving the balance of the nodule symbiosis (Murray et al., 2007; Mortier et al., 2010; Saur et al., 2011). Our study has experimentally confirmed one of those mechanisms, a negative role of NIN in rhizobial infection. Excessive root hair curling of a typical *nin* mutant also may be explained by our working model of NIN.

How can two different biological events, infection and organogenesis, be controlled by the same transcription factor, NIN? How can NIN act both positively and negatively in a stage- or tissue-dependent manner during nodule organogenesis? Recent reports in Arabidopsis indicate that a transcription factor may act as a bifunctional transcription factor and mediate a wide variety of biological events. WUSCHEL acts as both a repressor and an activator in a domain-dependent manner (Ikeda et al., 2009). In our study, however, a NIN chimeric repressor can repress IT formation in the epidermis (Fig. 5; Table I), so that NIN functions only as an activator in both infection and organogenesis. If NIN functions as a repressor of IT formation, the NIN chimeric repressor should not repress IT formation. Another possibility is that different actions of NIN are dependent on tissue- or stage-specific downstream targets, including cotranscriptional regulators. The putative cortex- or late nodule-specific downstream factors might suppress the function of NIN for IT formation transcriptionally or posttranscriptionally. This potential mechanism is supported by several studies. Studies of LEAFY and Activator protein1 transcription factors indicate that a single transcription factor can bind to different groups of targets by interacting with individual cis-regions or cofactors following the developmental stages (Gregis et al., 2008; Liu and Mara, 2010). Moreover, several reports of cross talk in defense signaling propose a potential mechanism by which single transcription factors, such as WRKYs and TGAs (bZIP-type transcription factor), play both positive roles in the salicylic acid-dependent pathway and negative roles in the jasmonic acid-dependent pathway (Li et al., 2004; Gao et al., 2011; Van der Does et al., 2013).

We next discuss the candidates for cofactors or downstream target genes of NIN. In terms of the cell proliferation activity of NIN, a positive role for organogenesis, the contribution of NSP2 and NF-YA/YB has been demonstrated (Soyano et al., 2013). For the negative regulation of infection, ethylene-responsive factors are strong candidates, given that both of the hyperinfection mutants, *Mtsickle* and *Medicago truncatula ethylene response factor required for nodule differentiation* (*Mtefd*), harbor mutations in ethylene-signaling molecules. Although a few hyperinfection mutants, *Ljhit1-1*, *Mtsickle*, and *Mtefd* (Penmetsa and Cook, 1997; Murray et al., 2007; Vernié et al., 2008), suggest the existence of regulatory mechanisms for controlling rhizobial infection processes, such regulation is far less well known than that of the number of nodules (van Brussel

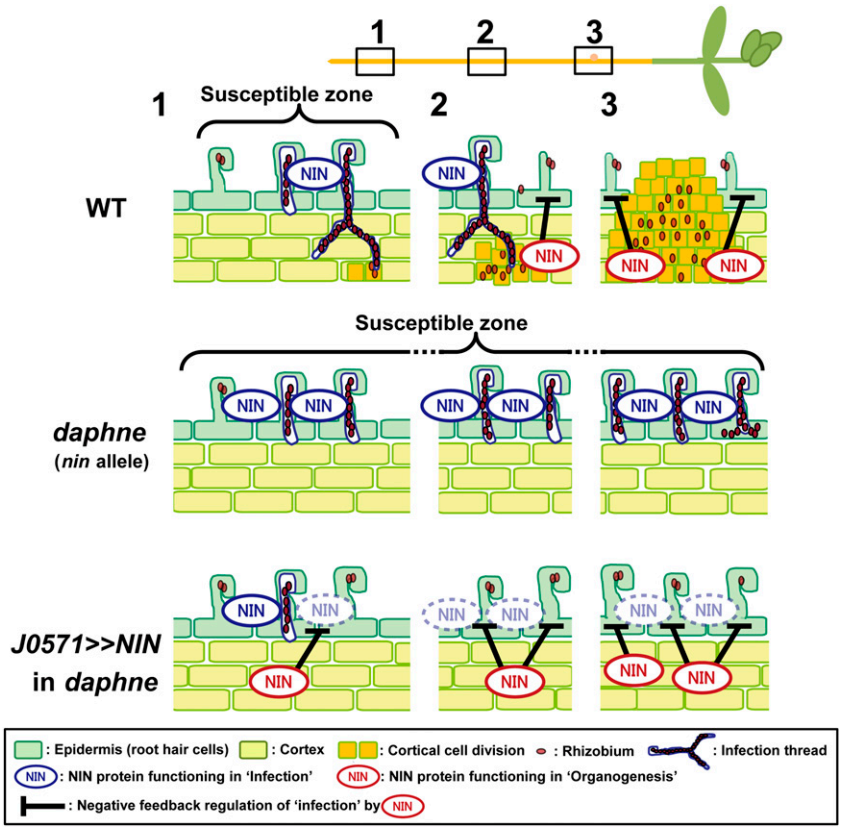


**Figure 7.** A model of the inhibition of rhizobial infection processes mediated by NIN. In the wild type (WT), NIN functions in both rhizobial infection (blue, in the epidermis) and organogenesis (red, in the cortex). In the earlier stage (1), NIN (blue) is predominant, but in the later stage (3), the proportion of NIN (red) has increased with nodule development. It is assumed that a potential negative correlation between the organogenesis and infection pathways (black bars) regulates the amount of infection and restricts the region of rhizobial susceptibility. In the *daphne* mutant, NIN functions only in infection (blue) and not in organogenesis (red), resulting in no activation of cortical cell division. The loss of NIN (red) enhances rhizobial infection. When we induced *NIN* expression in cortex in *daphne*, infection was strongly suppressed, owing to the loss of a negative feedback loop (black bars) mediated by NIN (red). The numbers indicate the developmental stages of nodulation. "NIN" surrounded by a dashed line indicates reduced gene expression or protein function of NIN, induced by the negative feedback loop described above (black bars).

et al., 2002; Oka-Kira and Kawaguchi, 2006; Kouchi et al., 2010). Furthermore, although *Ljhit1-1* exhibits low nodulation, *Mtsickle* and *Mtefd* exhibit increased numbers of nodules, leaving mysterious the putative cross talk between the infection and organogenesis pathways. According to our model, the phenotype of *Ljhit1-1* is caused by the lower expression of NIN functioning in organogenesis and inhibiting infection, similar to *daphne*. In contrast, in *Mtsickle* and *Mtefd*, NIN may be more highly expressed, but inhibitory mechanisms of infection mediated by NIN may be lost. Our study indicates that NIN may switch between positive and negative influence on rhizobial infection in different tissues or nodule developmental stages. NIN could be controlling the balance between infection and organogenesis. Future study of *daphne* will shed new light on the cofactors or downstream target genes of NIN that differ between those two pathways.

Although NIN is a key transcriptional factor in nodule development, the functional *NIN* promoter region necessary for nodule organogenesis has not yet been elucidated. Only IT formation, and not nodule formation, was rescued in *nin-9* by the introduction of *ProNIN(~4kb)*::*NIN*::*TerNIN* (Table I; Supplemental Fig. S5). In this study, we identified a novel mutant allele of *nin*, *daphne*, whose genome was changed approximately 7 kb upstream of *NIN* by chromosomal translocation (Fig. 2). These results raise at least two possibilities. One is that a cis-regulatory element necessary for the organogenesis pathway, including the cytokinin response element, has been lost from the upstream region of *NIN* in the *daphne* genome. In other words, a 7-kb segment of the *NIN* promoter region is sufficient for the function of NIN in the infection pathway. The other possibility is that epigenetic alteration leads to a different *NIN* expression pattern in *daphne*. Furthermore, *ProUBQ*::*NIN* induced aberrant roots including bumps in the wild type, *daphne*, and *nin-9* (Supplemental Fig. S6), but we failed to rescue IT formation in *nin-9* by the introduction of *ProUBQ*::*NIN* (Table I; Supplemental Fig. S5). This implies that the induction mechanism of *NIN* transcript is more complex than so far anticipated; spatial and temporal expression of *NIN* may need to be strictly controlled in order to achieve its functions in both infection and organogenesis pathways. The elucidation of the mechanism remains an important challenge.

The biological meaning of controlling the susceptibility of rhizobia has not been established. At least under our experimental conditions, *daphne* exhibited no difference in plant growth between the noninoculated and inoculated conditions (Supplemental Fig. S9). IT formation may be a less energy-consuming process than nodule formation or nitrogen fixation (van Brussel et al., 2002; Oka-Kira and Kawaguchi, 2006; Kouchi et al., 2010). Alternatively, it is possible that plants may need to avoid excessive bacterial infection even during an interaction with symbiotic bacteria. This may be related to a common mechanism for the establishment of plant-symbiont and plant-pathogen interactions (Vasse et al., 1993; Bozsó et al., 2009; Soto et al., 2009; Nakagawa et al., 2011).

Our study identified a novel *nin* mutant allele, *daphne*. We demonstrated that NIN, known to date as a positive factor for IT formation and nodule organogenesis, has a negative role in rhizobial infection processes. The multiple functions of the transcription factor NIN will afford an opportunity to investigate potential cross talk between infection in the epidermis and cell division in the cortex during the course of the establishment of nodule symbiosis.

## MATERIALS AND METHODS

### Plant Materials and Growth Conditions

The *daphne* mutant was isolated by screening M2 progeny derived from *Lotus japonicus* Miyakojima MG-20 wild-type seeds mutagenized by irradiation with a carbon ion beam ($C^{5+}$). The details of the ion beam irradiation have been reported previously (Oka-Kira et al., 2005; Magori et al., 2009; Yoshida et al., 2010). Seeds were sown in sterilized vermiculite soaked in autoclaved vermiculite supplied with Broughton and Dilworth solution (Broughton and Dilworth, 1971) containing 0.5 mM $KNO_3$ with or without *Mesorhizobium loti* MAFF 303099 under a 16-h-light/8-h-dark cycle. Cytokinin treatment was applied by incubation of seedlings in vermiculite supplied with Broughton and Dilworth solution containing $10^{-7}$ M benzylaminopurine for 16 h. ITs were observed or counted after inoculation of *M. loti* rhizobia constitutively expressing *LacZ* (Yoshida et al., 2010) or *DsRED*. *nin-2* was kindly provided by Jens Stougaard (Schauser et al., 1999) and was used for the allelism test. *nin-9* (Suzaki et al., 2012) was used for gene expression analysis and complementation testing.

### Microscopic Observation

Bright-field and fluorescence images were viewed with an SZX12/16 stereomicroscope or a BX50 microscope (Olympus). Images were acquired with a DP Controller (Olympus). Confocal images were viewed with an A1 confocal laser-scanning microscope (Nikon) and NIS Elements (Nikon).

### Quantification of ITs

At 5 d after germination, plants were inoculated with *M. loti* constitutively expressing *LacZ*. At 7 DAI, roots were stained for $\beta$-galactosidase activity. ITs on all parts of the root were counted using the microscope (BX50; Olympus).

### Map-Based Cloning and Inverse PCR

The *daphne* locus was mapped using F2 progeny of *daphne* and Gifu B-129. Two loci located on linkage groups II and III were identified using 52 F2 plants. Fine-mapping was performed in 2,048 F2 plants. The newly developed genetic markers in this study are shown in Supplemental Table S2. The deleted region located on CM0423 (chromosome III) was identified. *daphne* genomic DNA was extracted with the DNeasy Plant Mini Kit (Qiagen) and digested with *Eco*O109I, *Apo*I, and *Eco*RI. The digested DNA fragments were self-ligated with T4 DNA ligase (TaKaRa). Then, using inverse PCR analysis with two sets of primers designed on sequences in CM0423, the fused sequences originating from CM0423 (chromosome III) and CM0102 (chromosome II; Fig. 2) were detected. The primers used in inverse PCR analysis are shown in Supplemental Table S3.

### Expression Analysis

Total RNA was isolated from each plant tissue using the RNeasy Plant Mini Kit (Qiagen). First-strand cDNA was prepared using the QuantiTect Reverse Transcription Kit (Qiagen). Real-time RT-PCR was performed using the ABI Prism 7000 (Applied Biosystems) with THUNDERBIRD SYBR qPCR Mix (Toyobo) or with the QuanTitect SYBR Green RT-PCR Kit (Qiagen), according to each manufacturer's protocol. The expression of *ubiquitin* or *elongation factor-1$\alpha$* was used as the

reference. The primers used in expression analysis are shown in Supplemental Table S3. Data are means ± SD of three biological and three technical replicates.

## Plant Transformation

The recombinant plasmids were introduced into *Agrobacterium rhizogenes* strain AR1193 and were transformed into roots of *L. japonicus* by a hairy root transformation method described previously (http://www.bio-protocol.org/wenzhang.aspx?id=795; Okamoto et al., 2009).

## Cloning of *NIN* Promoter Constructs and Promoter-GUS Assay

A 1.7-kb Gateway cassette (GW) fragment was excised from the DR5 (for auxin-inducible reporter gene)::GFP-NLS construct (Suzaki et al., 2012) and inserted into the *Bam*HI site of pCAMBIA1300-GFP, named pCAMBIA1300-GW-GFP. Next, the *GFP* in the vector was removed using *Xho*I, and PCR-amplified *GFP-LjLTI6b* (Suzaki et al., 2012) was inserted into the *Xho*I site to create a new binary vector, pCAMBIA1300-GW-GFP-LjLTI6b. Then, using two sets of primers for the amplification of approximately 4 kb of *ProNIN* and approximately 2 kb of *TerNIN*, two fragments were cloned into pCAMBIA1300-GW-GFP-LjLTI6b. In the final step, *GUS* in pDONR221 (Invitrogen), which was provided by Detlef Weigel, and the *NIN* cDNA in pENTR/D-TOPO (Suzaki et al., 2012) were inserted between *ProNIN* and *TerNIN* by an LR recombination reaction (Invitrogen). A transfer DNA construct expressing *ProNIN*::*GUS*::*TerNIN* was transformed into MG-20 and *daphne*. GFP fluorescence was checked as a marker for transformation. Transformed roots were inoculated with *M. loti* MAFF303099. At 7 DAI, a GUS staining procedure was performed as described previously (Jefferson et al., 1987).

## Analysis of the IT Phenotype with Overexpressing NIN or a Chimeric Repressor of NIN

*NIN* cDNA without a stop codon in pENTR/D-TOPO was generated from *NIN* cDNA in pENTR/D-TOPO (Suzaki et al., 2012) by site-directed mutagenesis with primers (Supplemental Table S3). A *GW*::*SRDX* fragment was amplified from the pDEST-BCKH plasmid (Oshima et al., 2011) and inserted between the *Kpn*I and *Asc*I sites of pUB-GFP (Maekawa et al., 2008), named pUB-GW-SRDX-GFP. *NIN* cDNA in pENTR/D-TOPO (Suzaki et al., 2012) and *NIN* cDNA without a stop codon were inserted into the GW sites of pUB-GW-GFP (Maekawa et al., 2008) and pUB-GW-SRDX-GFP, respectively, with the LR recombination reaction (Invitrogen). As a control, *GUS* in pDONR221 (Invitrogen) was inserted into the GW site of pUB-GW-GFP by the LR recombination reaction (Invitrogen). *daphne* plants were treated with *M. loti* MAFF303099 constitutively expressing *DsRED*. At 14 DAI, ITs were observed.

## Analysis of Tissue Specificity Using a Cortex- and Endodermis-Specific Expression System

GAL4-VP16 (for herpes simplex virus protein) and the nopaline synthase (NOS) terminator sequence with flanking genomic regions were amplified by PCR from an enhancer trap line, J0571, in Arabidopsis (*Arabidopsis thaliana*; http://www.plantsci.cam.ac.uk/Haseloff/; Miyashima et al., 2011) and cloned into the *Hin*dIII site of pGWB501:5xUAS (Goh et al., 2012) using an In-Fusion HD cloning kit (TaKaRa), named pGWB501:5xUAS-J0571. Next, the *GW*::*SRDX*::*TerNOS* fragment was excised from pUB-GW-SRDX-GFP by *Kpn*I and *Sca*I double digestion and inserted into pCAMBIA1300-GFP, named pCAMBIA1300-GW-SRDX-GFP. A J0571-GAL4-VP16-TerNOS-5xUAS-35S minimal promoter was amplified by PCR from the template plasmid pGWB501:5xUAS-J0571 and inserted into the *Kpn*I site of pCAMBIA1300-GW-GFP or pCAMBIA1300-GW-SRDX-GFP, named pCAMBIA1300-J0571-GW-GFP or pCAMBIA1300-J0571-GW-SRDX-GFP, respectively. In the final step, *NIN* and *mCherry-NLS* coding sequence (Suzaki et al., 2012) or *NIN* and *mKusabira Orange2* (*mKO2*) coding sequence without a stop codon were inserted into the GW site of pCAMBIA1300-J0571-GW-GFP or pCAMBIA1300-J0571-GW-SRDX-GFP by the LR recombination reaction (Invitrogen). As a control, *mKO2* without a stop codon was amplified from the plasmid including *mKO2* (Medical and Biological Laboratories; Sakaue-Sawano et al., 2008) by PCR and cloned into pENTR/D-TOPO vector using a TOPO cloning kit (Invitrogen). Primers used for these constructs are listed in Supplemental Table S3. At 21 DAI, nodules and ITs were observed in transformed hairy roots.

## Supplemental Data

The following materials are available in the online version of this article.

**Supplemental Figure S1.** The phenotype of nodule formation in *hit1-1* mutant.

**Supplemental Figure S2.** *Z*-stack image series of same area of *daphne* root.

**Supplemental Figure S3.** The two loci responsible for nonnodulation of *daphne* by rough mapping.

**Supplemental Figure S4.** The result of complementation tests by the constitutive expression of *TIM*.

**Supplemental Figure S5.** Complementation of IT formation phenotype of *nin-9*.

**Supplemental Figure S6.** Enlarged bumps and tips were induced by overexpressing *NIN* in both MG-20 and *daphne*.

**Supplemental Figure S7.** Nodule organogenesis was decreased in *ProLjUBQ*::*NIN*::*SRDX*-expressing roots.

**Supplemental Figure S8.** The expression pattern of marker gene under the control of J0571 enhancer.

**Supplemental Figure S9.** The plant growth difference between noninoculated and inoculated conditions.

**Supplemental Table S1.** The segregation ratio of mapping population and backcrossing population.

**Supplemental Table S2.** The newly developed genetic markers list used for fine mapping in this study.

**Supplemental Table S3.** Primers used in this study.

## ACKNOWLEDGMENTS

We thank Jens Stougaard for the mutant seeds of *nin-2*, Krzyztof Szczyglowski for the mutant seeds of *hit1-1*, Detlef Weigel for the *GUS* construct, Makoto Hyashi for *M. loti* MAFF303099 expressing *DsRED*, Shusei Sato for the genomic data of *L. japonicus*, Masaru Ohme-Takagi for the *SRDX* construct, Masanao Sato and Kiyoshi Tatematsu for valuable comments, the Functional Genomics Facility and the Spectrography and Bioimaging Facility of the National Institute for Basic Biology Core Research Facilities and the Model Plant Facilities of the National Institute for Basic Biology Bioresource Center for technical support, and Enago (www.enago.jp) for the English language review.

Received December 2, 2013; accepted April 8, 2014; published April 10, 2014.

## LITERATURE CITED

**Borisov AY, Madsen LH, Tsyganov VE, Umehara Y, Voroshilova VA, Batagov AO, Sandal N, Mortensen A, Schauser L, Ellis N, et al** (2003) The *Sym35* gene required for root nodule development in pea is an ortholog of *Nin* from *Lotus japonicus*. Plant Physiol **131:** 1009–1017

**Bozsó Z, Maunoury N, Szatmari A, Mergaert P, Ott PG, Zsíros LR, Szabó E, Kondorosi E, Klement Z** (2009) Transcriptome analysis of a bacterially induced basal and hypersensitive response of *Medicago truncatula*. Plant Mol Biol **70:** 627–646

**Broughton WJ, Dilworth MJ** (1971) Control of leghaemoglobin synthesis in snake beans. Biochem J **125:** 1075–1080

**Crespi M, Frugier F** (2008) De novo organ formation from differentiated cells: root nodule organogenesis. Sci Signal **1:** re11

**Fournier J, Timmers ACJ, Sieberer BJ, Jauneau A, Chabaud M, Barker DG** (2008) Mechanism of infection thread elongation in root hairs of *Medicago truncatula* and dynamic interplay with associated rhizobial colonization. Plant Physiol **148:** 1985–1995

**Gage DJ** (2004) Infection and invasion of roots by symbiotic, nitrogen-fixing rhizobia during nodulation of temperate legumes. Microbiol Mol Biol Rev **68:** 280–300

**Gao QM, Venugopal S, Navarre D, Kachroo A** (2011) Low oleic acid-derived repression of jasmonic acid-inducible defense responses requires the WRKY50 and WRKY51 proteins. Plant Physiol **155:** 464–476

**Goh T, Joi S, Mimura T, Fukaki H** (2012) The establishment of asymmetry in *Arabidopsis* lateral root founder cells is regulated by LBD16/ASL18 and related LBD/ASL proteins. Development **139:** 883–893

**Gonzalez-Rizzo S, Crespi M, Frugier F** (2006) The *Medicago truncatula* CRE1 cytokinin receptor regulates lateral root development and early symbiotic interaction with *Sinorhizobium meliloti*. Plant Cell **18:** 2680–2693

**Gregis V, Sessa A, Colombo L, Kater MM** (2008) AGAMOUS-LIKE24 and SHORT VEGETATIVE PHASE determine floral meristem identity in Arabidopsis. Plant J **56:** 891–902

**Heckmann AB, Sandal N, Bek AS, Madsen LH, Jurkiewicz A, Nielsen MW, Tirichine L, Stougaard J** (2011) Cytokinin induction of root nodule primordia in *Lotus japonicus* is regulated by a mechanism operating in the root cortex. Mol Plant Microbe Interact **24:** 1385–1395

**Ikeda M, Mitsuda N, Ohme-Takagi M** (2009) *Arabidopsis* WUSCHEL is a bifunctional transcription factor that acts as a repressor in stem cell regulation and as an activator in floral patterning. Plant Cell **21:** 3493–3505

**Jefferson RA, Kavanagh TA, Bevan MW** (1987) GUS fusions: beta-glucuronidase as a sensitive and versatile gene fusion marker in higher plants. EMBO J **6:** 3901–3907

**Jones KM, Kobayashi H, Davies BW, Taga ME, Walker GC** (2007) How rhizobial symbionts invade plants: the *Sinorhizobium-Medicago* model. Nat Rev Microbiol **5:** 619–633

**Kosuta S, Held M, Hossain MS, Morieri G, Macgillivary A, Johansen C, Antolín-Llovera M, Parniske M, Oldroyd GED, Downie AJ, et al** (2011) *Lotus japonicus symRK-14* uncouples the cortical and epidermal symbiotic program. Plant J **67:** 929–940

**Kouchi H, Imaizumi-Anraku H, Hayashi M, Hakoyama T, Nakagawa T, Umehara Y, Suganuma N, Kawaguchi M** (2010) How many peas in a pod? Legume genes responsible for mutualistic symbioses underground. Plant Cell Physiol **51:** 1381–1397

**Krusell L, Madsen LH, Sato S, Aubert G, Genua A, Szczyglowski K, Duc G, Kaneko T, Tabata S, de Bruijn F, et al** (2002) Shoot control of root development and nodulation is mediated by a receptor-like kinase. Nature **420:** 422–426

**Li J, Brader G, Palva ET** (2004) The WRKY70 transcription factor: a node of convergence for jasmonate-mediated and salicylate-mediated signals in plant defense. Plant Cell **16:** 319–331

**Liu ZC, Mara C** (2010) Regulatory mechanisms for floral homeotic gene expression. Semin Cell Dev Biol **21:** 80–86

**Madsen LH, Tirichine L, Jurkiewicz A, Sullivan JT, Heckmann AB, Bek AS, Ronson CW, James EK, Stougaard J** (2010) The molecular network governing nodule organogenesis and infection in the model legume *Lotus japonicus*. Nat Commun **1:** 10

**Maekawa T, Kusakabe M, Shimoda Y, Sato S, Tabata S, Murooka Y, Hayashi M** (2008) Polyubiquitin promoter-based binary vectors for overexpression and gene silencing in *Lotus japonicus*. Mol Plant Microbe Interact **21:** 375–382

**Magori S, Oka-Kira E, Shibata S, Umehara Y, Kouchi H, Hase Y, Tanaka A, Sato S, Tabata S, Kawaguchi M** (2009) *Too much love*, a root regulator associated with the long-distance control of nodulation in *Lotus japonicus*. Mol Plant Microbe Interact **22:** 259–268

**Marsh JF, Rakocevic A, Mitra RM, Brocard L, Sun J, Eschstruth A, Long SR, Schultze M, Ratet P, Oldroyd GED** (2007) *Medicago truncatula NIN* is essential for rhizobial-independent nodule organogenesis induced by autoactive calcium/calmodulin-dependent protein kinase. Plant Physiol **144:** 324–335

**Miyashima S, Koi S, Hashimoto T, Nakajima K** (2011) Non-cell-autonomous microRNA165 acts in a dose-dependent manner to regulate multiple differentiation status in the Arabidopsis root. Development **138:** 2303–2313

**Mortier V, Den Herder G, Whitford R, Van de Velde W, Rombauts S, D'Haeseleer K, Holsters M, Goormachtig S** (2010) CLE peptides control *Medicago truncatula* nodulation locally and systemically. Plant Physiol **153:** 222–237

**Murray JD** (2011) Invasion by invitation: rhizobial infection in legumes. Mol Plant Microbe Interact **24:** 631–639

**Murray JD, Karas BJ, Sato S, Tabata S, Amyot L, Szczyglowski K** (2007) A cytokinin perception mutant colonized by Rhizobium in the absence of nodule organogenesis. Science **315:** 101–104

**Nakagawa T, Kaku H, Shimoda Y, Sugiyama A, Shimamura M, Takanashi K, Yazaki K, Aoki T, Shibuya N, Kouchi H** (2011) From defense to symbiosis: limited alterations in the kinase domain of LysM receptor-like kinases are crucial for evolution of legume-*Rhizobium* symbiosis. Plant J **65:** 169–180

**Oka-Kira E, Kawaguchi M** (2006) Long-distance signaling to control root nodule number. Curr Opin Plant Biol **9:** 496–502

**Oka-Kira E, Tateno K, Miura K, Haga T, Hayashi M, Harada K, Sato S, Tabata S, Shikazono N, Tanaka A, et al** (2005) *klavier* (*klv*), a novel hypernodulation mutant of *Lotus japonicus* affected in vascular tissue organization and floral induction. Plant J **44:** 505–515

**Okamoto S, Ohnishi E, Sato S, Takahashi H, Nakazono M, Tabata S, Kawaguchi M** (2009) Nod factor/nitrate-induced *CLE* genes that drive HAR1-mediated systemic regulation of nodulation. Plant Cell Physiol **50:** 67–77

**Oldroyd GED** (2013) Speak, friend, and enter: signalling systems that promote beneficial symbiotic associations in plants. Nat Rev Microbiol **11:** 252–263

**Op den Camp RH, De Mita S, Lillo A, Cao Q, Limpens E, Bisseling T, Geurts R** (2011) A phylogenetic strategy based on a legume-specific whole genome duplication yields symbiotic cytokinin type-A response regulators. Plant Physiol **157:** 2013–2022

**Oshima Y, Mitsuda N, Nakata M, Nakagawa T, Nagaya S, Kato K, Ohme-Takagi M** (2011) Novel vector systems to accelerate functional analysis of transcription factors using chimeric repressor gene-silencing technology (CRES-T). Plant Biotechnol **28:** 201–210

**Penmetsa RV, Cook DR** (1997) A legume ethylene-insensitive mutant hyperinfected by its rhizobial symbiont. Science **275:** 527–530

**Popp C, Ott T** (2011) Regulation of signal transduction and bacterial infection during root nodule symbiosis. Curr Opin Plant Biol **14:** 458–467

**Radutoiu S, Madsen LH, Madsen EB, Felle HH, Umehara Y, Grønlund M, Sato S, Nakamura Y, Tabata S, Sandal N, et al** (2003) Plant recognition of symbiotic bacteria requires two LysM receptor-like kinases. Nature **425:** 585–592

**Rival P, de Billy F, Bono JJ, Gough C, Rosenberg C, Bensmihen S** (2012) Epidermal and cortical roles of *NFP* and *DMI3* in coordinating early steps of nodulation in *Medicago truncatula*. Development **139:** 3383–3391

**Sakaue-Sawano A, Ohtawa K, Hama H, Kawano M, Ogawa M, Miyawaki A** (2008) Tracing the silhouette of individual cells in S/G2/M phases with fluorescence. Chem Biol **15:** 1243–1248

**Sandal N, Petersen TR, Murray J, Umehara Y, Karas B, Yano K, Kumagai H, Yoshikawa M, Saito K, Hayashi M, et al** (2006) Genetics of symbiosis in *Lotus japonicus*: recombinant inbred lines, comparative genetic maps, and map position of 35 symbiotic loci. Mol Plant Microbe Interact **19:** 80–91

**Saur IML, Oakes M, Djordjevic MA, Imin N** (2011) Crosstalk between the nodulation signaling pathway and the autoregulation of nodulation in Medicago truncatula. New Phytol **190:** 865–874

**Schauser L, Roussis A, Stiller J, Stougaard J** (1999) A plant regulator controlling development of symbiotic root nodules. Nature **402:** 191–195

**Soto MJ, Domínguez-Ferreras A, Pérez-Mendoza D, Sanjuán J, Olivares J** (2009) Mutualism versus pathogenesis: the give-and-take in plant-bacteria interactions. Cell Microbiol **11:** 381–388

**Soyano T, Kouchi H, Hirota A, Hayashi M** (2013) Nodule inception directly targets *NF-Y* subunit genes to regulate essential processes of root nodule development in *Lotus japonicus*. PLoS Genet **9:** e1003352

**Suzaki T, Yano K, Ito M, Umehara Y, Suganuma N, Kawaguchi M** (2012) Positive and negative regulation of cortical cell division during root nodule development in *Lotus japonicus* is accompanied by auxin response. Development **139:** 3997–4006

**Tirichine L, Sandal N, Madsen LH, Radutoiu S, Albrektsen AS, Sato S, Asamizu E, Tabata S, Stougaard J** (2007) A gain-of-function mutation in a cytokinin receptor triggers spontaneous root nodule organogenesis. Science **315:** 104–107

**van Brussel AAN, Tak T, Boot KJM, Kijne JW** (2002) Autoregulation of root nodule formation: signals of both symbiotic partners studied in a split-root system of *Vicia sativa* subsp. *nigra*. Mol Plant Microbe Interact **15:** 341–349

**Van der Does D, Leon-Reyes A, Koornneef A, Van Verk MC, Rodenburg N, Pauwels L, Goossens A, Körbes AP, Memelink J, Ritsema T, et al** (2013) Salicylic acid suppresses jasmonic acid signaling downstream of $SCF^{COI1}$-JAZ by targeting GCC promoter motifs via transcription factor ORA59. Plant Cell **25:** 744–761

**Vasse J, Debilly F, Truchet G** (1993) Abortion of infection during the *Rhizobium meliloti*-alfalfa symbiotic interaction is accompanied by a hypersensitive reaction. Plant J **4:** 555–566

**Vasse JM, Truchet GL** (1984) The *Rhizobium*-legume symbiosis: observation of root infection by bright-field microscopy after staining with methylene blue. Planta **161:** 487–489

**Vernié T, Moreau S, de Billy F, Plet J, Combier JP, Rogers C, Oldroyd G, Frugier F, Niebel A, Gamas P** (2008) EFD is an ERF transcription factor involved in the control of nodule number and differentiation in *Medicago truncatula*. Plant Cell **20:** 2696–2713

**Yoshida C, Funayama-Noguchi S, Kawaguchi M** (2010) *plenty*, a novel hypernodulation mutant in *Lotus japonicus*. Plant Cell Physiol **51:** 1425–1435